THE JOURNAL OF BIOLOGICAL CHEMISTRY
Vol. 273, No. 3, Issue of January 16, pp. 1596–1604, 1998

Printed in U.S.A.

Crystal Structure of a Calcium-Phospholipid Binding Domain from Cytosolic Phospholipase A2*

(Received for publication, September 24, 1997)

Olga Perisic‡, Sun Fong§, Denise E. Lynch‡, Mark Bycroft§, and Roger L. Williams‡¶

From the ‡Medical Research Council Laboratory of Molecular Biology and §Centre for Protein Engineering, Medical Research Council Centre, Hills Road, Cambridge CB2 2QH, United Kingdom

Cytosolic phospholipase A2 (cPLA2) is a calcium-sensitive 85-kDa enzyme that hydrolyzes arachidonic acid-containing membrane phospholipids to initiate the biosynthesis of eicosanoids and platelet-activating factor, potent inflammatory mediators. The calcium-dependent activation of the enzyme is mediated by an N-terminal C2 domain, which is responsible for calcium-dependent translocation of the enzyme to membranes and that enables the intact enzyme to hydrolyze membrane-resident substrates. The 2.4-Å x-ray crystal structure of this C2 domain was solved by multiple isomorphous replacement and reveals a β-sandwich with the same topology as the C2 domain from phosphoinositide-specific phospholipase Cδ1. Two clusters of exposed hydrophobic residues surround two adjacent calcium binding sites. This region, along with an adjoining strip of basic residues, appear to constitute the membrane binding motif. The structure provides a striking insight into the relative importance of hydrophobic and electrostatic components of membrane binding for cPLA2. Although hydrophobic interactions predominate for cPLA2, for other C2 domains such as in "conventional" protein kinase C and synaptotagmins, electrostatic forces prevail.

Mammalian phospholipases A2 (PLA2s)[1] are a large superfamily of enzymes with a common function of catalyzing the release of fatty acid from the *sn*-2 position of membrane phospholipids, but with distinct structural and biochemical characteristics and different roles in signal transduction and general lipid metabolism (reviewed in Refs. 1–3). Cytosolic PLA2 (cPLA2) is an 85-kDa protein with no sequence homology to any other PLA2s (Refs. 4 and 5; reviewed in Refs. 3 and 6–8). This enzyme preferentially hydrolyzes phospholipids containing arachidonate at the *sn*-2 position, thus providing free arachidonic acid for the biosynthesis of eicosanoides, potent inflammatory lipid mediators. cPLA2 is found in a variety of cells where it can act as a receptor-regulated enzyme that can mediate agonist-induced arachidonic acid release (9, 10). cPLA2 is activated by low levels of calcium (11–14), but calcium is not directly involved in catalysis and is required only for membrane binding (15, 16). The enzyme translocates from cytosol to membranes in the presence of physiologically relevant, submicromolar calcium levels (5, 17, 18). The increase in intracellular calcium triggered by calcium ionophores or agonists such as histamine, thrombin, bradykinin, or IgE/antigen causes the translocation of the enzyme from the cytosol to the nuclear membrane and endoplasmic reticulum (19–22). Interestingly, a number of enzymes involved in eicosanoid metabolism, such as prostaglandin endoperoxide synthase 1 and 2, 5-lipoxygenase, and 5-lipoxygenase-activating protein also localize to the nuclear envelope and endoplasmic reticulum (19, 23). In addition to calcium, the activation of cPLA2 by some agonists requires phosphorylation of the enzyme (7, 8).

Using limited proteolysis and deletion analysis, two functionally distinct domains have been mapped in cPLA2: an N-terminal domain responsible for Ca^{2+}-dependent phospholipid binding known as a CaLB or a C2 domain and a C-terminal, Ca^{2+}-independent catalytic domain capable of hydrolyzing monomeric substrates but unable to associate with membranes (16).

In this paper, we describe the crystal structure and calcium binding characteristics of the N-terminal domain of cPLA2 that is responsible for Ca^{2+}-dependent translocation and membrane binding of the enzyme. The structure accounts for the observed preference of cPLA2 for phospholipids with hydrophobic features such as phosphatidylcholine and explains previous observations suggesting the importance of the hydrophobic forces involved in binding of the cPLA2 C2 domain to phospholipid membranes (15, 24, 25). Implications for the relative contributions of the hydrophobic/electrostatic interactions in the membrane binding of the C2 domains from other well characterized proteins are also presented.

EXPERIMENTAL PROCEDURES

Cloning and Expression—DNA fragments encoding residues 1–137, 1–141, or 17–141 of human cPLA2 were amplified by polymerase chain reaction using a plasmid containing the gene for the intact enzyme that was generously provided by Zeneca Pharmaceuticals, Macclesfield, UK. The *Bgl*II site was incorporated at the 5′ end of the coding sequence and an *Eco*RI site followed by a stop codon was incorporated at the 3′ end to enable cloning into *Bam*HI and *Eco*RI-cut vector mini-pRSETA. This vector is a version of pRSETA (Invitrogen) modified so to encode a 17-residue N-terminal tail (MRGSHHHHHHGLVPRGS) containing a His_6 tag for affinity purification and a thrombin cleavage site rather than the original enterokinase cleavage site for the tag removal.[2] The expressed proteins after thrombin cleavage retain at their N terminus two additional amino acids (Gly-Ser) encoded by the vector. In addition to this deviation from the native sequence, constructs 1–141 and 17–141 have two substitutions at their C terminus, C139A and C141S, that were introduced to eliminate possible complications that could be caused by cysteine residues during the refolding procedure (see below). For the purpose of heavy atom derivatives, a construct was made with a substitution of only one of these cysteines (C141S) while preserving the other cysteine (Cys-139). The proteins were expressed in *Esche-*

* The costs of publication of this article were defrayed in part by the payment of page charges. This article must therefore be hereby marked "*advertisement*" in accordance with 18 U.S.C. Section 1734 solely to indicate this fact.

The atomic coordinates and structure factors (code 1RLW) have been deposited in the Protein Data Bank, Brookhaven National Laboratory, Upton, NY.

¶ To whom correspondence should be addressed: Tel.: 44-1223-402171; Fax: 44-1223-412178; E-mail: rlw@mrc-lmb.cam.ac.uk.

[1] The abbreviations used are: PLA2, phospholipase A2; cPLA2, cytosolic PLA2; PLC, phospholipase C; CBR, calcium binding region; PI, phosphatidylinositol; PKC, protein kinase C; MARCKS, myristoylated alanine-rich protein kinase C substrate.

[2] M. Proctor and M. Bycroft, unpublished data.

TABLE I
Statistics for crystallographic data collection and phase refinement

Diffraction data

Data set	X-ray source	Wavelength	d_{min}	Measurements	Unique reflections	Completeness	R_{merge}[a]
		Å	*Å*			%	%
Native (1)	BW7B	0.88	2.4	52266	11798	99.7	8.6
Native (2)	SRS 7.2	1.488	2.7	34681	7128	99.0	8.0
K_2PtCl_4 (1)	SRS 9.6	0.88	3.8	7690	4697	88.8	15.8
K_2PtCl_4 (2)	SRS 9.6	0.88	3.1	14964	4889	97.2	8.4
$LaCl_3$	BW7B	0.88	2.5	43754	9142	99.5	7.4

Multiple isomorphous replacement phase determination

Data set[b]	R_{iso}[c]	Sites	R_{cullis}[d]	Resolution	Phasing power		
					Isomorphous		Anomalous
					Centric	Acentric	
	%			*Å*			
Native (2)	15.3	2Ca/2Cd	0.92	2.8	0.66	1.1	1.5
K_2PtCl_4 (1)	43.0	2Ca/2Cd/1Pt	0.92	3.8	1.0	1.4	0.43
K_2PtCl_4 (2)	38.3	2Ca/2Cd/1Pt	0.89	3.1	1.2	1.4	0.66
$LaCl_3$	21.1	2La/2Cd	0.84	2.5	1.0	1.3	1.1

[a] $R_{merge} = \Sigma_{hkl}\Sigma_i|I_i(hkl) - \langle I(hkl)\rangle|/\Sigma_{hkl}\Sigma_i\ I_i(hkl)$.
[b] All of the data sets contain the $CaCl_2$ and $CdSO_4$ that were present in the crystallization setup. The native (1) data set was taken as the native data set for the purpose of heavy atom refinement in SHARP, whereas native (2) was treated as a derivative data set in the SHARP refinement.
[c] $R_{iso} = \Sigma\ ||F_{deriv}| - |F_{native}||/\Sigma\ |F_{native}|$.
[d] $R_{Cullis} = \Sigma\ ||F_{PH} \pm F_P| - F_{H(calc)}|/\Sigma\ |F_{PH} \pm F_P|$, shown for isomorphous, acentric differences.

richia coli BLR(DE3) (Novagen). Cells were grown at 37 °C, induced at an $A_{600} \sim 0.5$ with 0.5 mM isopropyl-1-thio-β-D-galactopyranoside at 25 °C for 12 h, and harvested by centrifugation.

Purification and Refolding—The insoluble fraction containing the fusion protein was isolated from 0.5 liters of cells by sonication and centrifugation. The pellets were solubilized in 8 M urea, Tris-HCl, pH 7.2, for 2 h at room temperature and centrifuged to remove the insoluble debris, and the denatured fusion protein was bound to 10 ml of Ni^{2+}-nitrilotriacetic acid-agarose (Qiagen) equilibrated in the same buffer. After washing the column with several column volumes of 8 M urea-Tris buffer, the protein was eluted with 300 mM imidazole in the 8 M urea-Tris buffer, concentrated with Centriprep 10 to 1 ml, and renatured by slow dilution into a rapidly stirred solution of 1.5 M urea, 50 mM Tris-HCl, pH 7.2. The solution was left at room temperature for 1 h and then dialyzed against 50 mM Tris-HCl, pH 8.0. The protein was concentrated using a Centriprep 10 and passed through a gel filtration Superdex 75 16/60 column (Pharmacia), equilibrated in 50 mM Tris-HCl, pH 8.0. The peak of the monomeric, refolded protein was cleaved with ~50 units of thrombin/milligram of protein at 4 °C to remove the tag. The sample was further purified by chromatography on a MonoQ 10/10 column equilibrated in 50 mM Tris-HCl, pH 8.0, and eluted with a gradient of sodium chloride. Protein was concentrated to ~18 mg/ml and stored at 4 °C.

Crystallization —The crystals were grown at 21 °C in hanging drops by the vapor diffusion method. Protein (5–10 mg/ml) was first incubated with 5 mM calcium chloride for at least 30 min and then mixed with an equal volume of a precipitant containing 1 M sodium acetate, 0.1 M Hepes, pH 7.5, and 50 mM $CdSO_4$. Crystals appeared after 1 week and slowly grew over 3 weeks to about 0.05 × 0.05 × 0.5 mm. Crystals had $P3_121$ symmetry with $a = 79.41$ and $c = 70.67$.

Diffraction Data Collection—For data collection, crystals were flash-frozen in nylon loops using a nitrogen gas stream at 100 K. For the freezing, crystals were briefly transferred to a cryoprotectant solution consisting of 66 mM Hepes, pH 7.5, 660 mM sodium acetate, 33 mM $CdSO_4$, and 25% (v/v) glycerol. Table I summarizes the data sets collected. Each data set was collected from a single crystal and processed using the program MOSFLM (26). The protein with a double cysteine substitution (C139A,C141S) was used for all the data sets except for the K_2PtCl_4 (I) derivative data set for which a protein with a single cysteine substitution (C141S) was used. For the heavy atom derivatives, crystals were soaked for 20 h in the reservoir solution containing 1 mM K_2PtCl_4 (data set K2PtCl$_4$ (I)) for 5 h in 5 mM K_2PtCl_4 (data set K2PtCl$_4$ (II)) or for 4 h in 10 mM $LaCl_3$. Crystals were also grown in the presence of 10 mM L-α-glycerophosphocholine or L-α-glycerophosphoserine, but no density corresponding to these compounds was observed.

Structure Solution—Most crystallographic calculations were carried out using the Collaborative Computing Project Number 4 (CCP4) program suite (27). Molecular replacement using either PLC-δ1-C2 (2ISD) or SytIA-C2 (1RSY) located a single molecule in the asymmetric unit; however, several loops were impossible to trace, and extensive efforts to build and refine a model using the molecular replacement phases proved unsuccessful. Consequently, several heavy atom derivative data sets were collected. One platinum site was located by a Patterson map search using the program SHELX (28). Other sites for other derivatives were located by difference Fourier analysis. Using the platinum and lanthanum derivative-phased multiple isomorphous replacement map, two strong peaks were located at the same position for all data sets. These sites were interpreted as cadmium sites. The program SHARP (29) was used to refine all heavy atom parameters using both anomalous and isomorphous differences. The MIRAS map showed only one molecule in the asymmetric unit. Following solvent flattening with the program SOLOMON (30) using a solvent content of 76%, the electron density was easily interpretable, and a model was built using the program O (31) and refined with the program REFMAC (32) using all data between 15 Å and 2.4 Å (9,339 reflections). The final conventional R-factor was 22.8% with a free R-factor of 27.2% (based on 1,003 random reflections in thin shells of resolution) for a model consisting of 1,001 protein atoms, 151 waters, two calcium ions, and two cadmiums. The average B-factor was 28 $Å^2$. The r.m.s. deviations from ideal geometry were 0.007 Å and 1.8° for bond lengths and bond angles. According to analysis by PROCHECK (33), 86% of residues are in the most favorable regions of the Ramachandran plot, and none are in disallowed areas. The overall average G-factor from PROCHECK was −0.08. In the final SIGMAA-weighted 2 $m|F_o|-D|F_C|$ electron density map (34), there is no break in the main chain density contoured at 1.2σ.

The model showed that the molecular replacement solution had correctly placed the β-sheets, but some loop conformations, particularly calcium binding region 1 (CBR1) and strand β7, were greatly different than those in either PLCδ-C2 or SytI-C2A. In addition, the structure showed a shift in the sequence alignment for the last two β strands relative to the alignment that was expected on the basis of sequence analysis (35). The platinum derivatives each had a single site corresponding to an interaction with the side chain of Met-98. The two cadmium sites each have ligands from two adjacent molecules in the crystal and appear to be essential for crystal packing. The refined B-factors of the calcium ions were considerably lower than their surrounding protein ligands, suggesting partial occupancy of these sites by more electron-dense cadmium. This was confirmed by collecting a 2.5-Å resolution data set in which crystals were soaked in a solution with a much greater concentration of calcium (40 mM) and a lower concentration of cadmium (10 mM). For this data set, the B-factors of the calcium were approximately the same as their protein ligands.

The coordinates and structure factor amplitudes will be deposited with the Protein Data Bank and can be obtained immediately via E-mail to the author.

RESULTS AND DISCUSSION

The Domain Boundaries for the cPLA2 C2 Domain—To pursue structural studies of the isolated cPLA2 C2 domain, we made several constructs with slightly different boundaries for the expression in *E. coli*. Two topologies for C2 domains have been described: one present in the first C2 domain of synaptotagmin I (SytI-C2A) (36) (S variant or topology I) and another present in the phosphoinositide-specific phospholipase C (PLCδ-C2) (37) (P variant or topology II) (35, 38). The two topologies can be best described as circular permutations of each other. PLC-δ1 starts with a strand corresponding to the β2 strand of (SytI-C2A) and ends with a strand corresponding to the β1 strand of SytI-C2A. Choosing wrong boundaries for the isolated domain could greatly destabilize the protein by truncating either the N-terminal or the C-terminal strand.

Three constructs were expressed that would cover either the S variant (amino acids 1–137) or the P variant (amino acids 17–141) or both topologies (amino acids 1–141). When expressed in *E. coli*, all three constructs were insoluble and had to be refolded from inclusion bodies. Among the three constructs, 17–141 was the most stable (determined from temperature denaturation monitored by circular dichroism and equilibrium urea denaturation monitored by fluorescence[3]) and was the only one that yielded crystals in the crystallization trials.

The Overall Fold—The overall fold of the cPLA2 C2 domain is illustrated in Fig. 1*A*. As with the C2 domain from PLC-δ1 (PLCδ-C2) and the C2A domain from Syt I (SytI-C2A), it consists of an anti-parallel β-sandwich with two 4-stranded sheets. Sheet I of the β-sandwich consisting of strands 3, 2, 5, and 6 and has a concave surface to it, whereas sheet II has a convex appearance. The topology of the domain is identical to that of PLCδ-C2 and is a circular permutation of the SytI-C2A topology (Fig. 2). Recently, this topology was predicted for the cPLA2 C2 domain based on the sequence analysis of 65 C2 domains and the known structure for the two topological variants (35). Although naturally occurring circular permutations have been noted previously for other proteins (39), the C2 domains have strikingly conserved three-dimensional structures despite the topological variations. A structurally conserved core of 105 residues of the C2 domain of cPLA2 can be superimposed on those of PLC-δ1-C2 and SytI-C2A with 1.3 and 1.4 Å r.m.s. deviation, respectively. As shown in Fig. 2, the residues that superimpose well among the three C2 domains are two of the connecting loops (CBR2 and CBR3) and all of the β-strands except the edge strand 7 of sheet II. Two loops involved in calcium binding, CBR2 and CBR3, have main-chain conformations that are essentially identical to the conformations observed for PLCδ-C2 and for SytIA-C2. The third loop involved in calcium binding, CBR1, is longer than in either PLC-δ1 or SytI-C2A and has a turn of α-helix. Among the three C2 domain structures, CBR1 has the most variable loop conformation. From sequence analysis of C2 domains, it is clear that this region has the greatest variability in both length and character (35, 40). The curved shape of the domain is caused by four β-bulges that represent a conserved feature of the cPLA2, SytI-C2A, and PLCδ-C2 domains.

Calcium Binding to cPLA2 C2 Domain—The C2 domain of cPLA2 was co-crystallized with calcium, and the structure reveals that it binds two Ca^{2+} ions at one end of the domain between three loops, previously named CBRs: CBR1, CBR2, and CBR3 (Fig. 1*B*, Fig. 2) (38). As with PLCδ-C2, the two calcium sites are adjacent and about 4 Å apart. Calcium site I has a coordination that is approximately a pentagonal bipyramid with one of the equatorial positions missing where the two sites adjoin each other. The coordination at site II is best described as an octahedron with one of the equatorial vertices represented by a bidentate interaction with Asp-93. Calcium site I has six ligands with an average distance to the calcium of 2.5 Å and consists of one side-chain oxygen from each of Asp-40, Asp-43, Asn-65, the carbonyl oxygen of Thr-41, and two water molecules (Fig. 1, Fig. 3). The seven ligands for site II have an average distance to the calcium of 2.5 Å and consist of one side-chain oxygen from each of Asp-40, Asp-43, and Asn-95, both side-chain oxygens of Asp-93, the carbonyl oxygen of Ala-94, and one water molecule. The exposed apices of each calcium site are occupied by waters (Fig. 1*C*). These waters would presumably be displaced so that the calcium ions could form a direct interaction with the phosphate moiety of a lipid headgroup. Two of the residues ligating the Ca^{2+} ions, Asp-40 and Asp-43, form one interaction with each Ca^{2+} ion. This arrangement of Ca^{2+} binding sites would be expected to lead to cooperative Ca^{2+} binding because the binding of one ion would position the ligands of the second ion as well as neutralize the negative charge in the binding site, allowing the acidic side chains for the second site to more closely approach each other.

Taken together, the structural studies of C2 domains suggest three possible Ca^{2+} binding sites, I, II, and III (Fig. 3). SytI-C2A shows Ca^{2+} binding in sites II and III (41) and PLCδ-C2 binding in sites I and II (and in all three sites with lanthanum) (38, 42). The two sites in cPLA2 correspond to sites I and II. The structural arrangement of these multiple sites explains the cooperativity of calcium binding that has been observed. A Hill coefficient of 3 has been reported for the isolated SytI-C2A domain (43), the Doc2β C2A domain (44), the SytII-C2A domain, (45) and for the C2 domain from PKC-β (41). Half-maximal binding of these domains to phosphatidylcholine /phosphatidylserine lyposomes occurs at very similar, 1–5 μM, free calcium concentrations. In the absence of phospholipids, the affinity for calcium is much lower, and dissociation constants of 60 μM (site II) and 400 μM (site III) for calcium binding to the SytIA domain have been reported (41). The lack of calcium binding at site III in the cPLA2 C2 domain is likely due to the conservative substitution D95N in comparison with the analogous CBR3 residue of SytI-C2A (Asp-232) and PLC-δ1 (Asp-708). This would further decrease the already low affinity in Site III (400 μM) as measured for SytI-C2A. The equivalent mutation in SytI-C2A (D232N) abolishes calcium-dependent phospholipid binding (46), whereas in the SytII-C2A it (D231N) causes a switch from the high affinity to low affinity calcium-dependent phospholipid binding (45).

CBR1 is among the most flexible parts of the PLC-δ1 and SytI-C2A domains. Multiple conformations of this loop were observed for PLC-δ1. For both PLC-δ1 and SytI-C2A, this region is characterized by generally higher temperature factors as well as some main-chain disorder (36, 38, 41, 42). In the presence of a metal, limited stabilization of CBR1 conformation has been observed in PLC-δ1 crystals (38, 42) and for SytI-C2A in solution (41). In cPLA2, CBR1 does not have unusually large temperature factors, and there is no disorder in it apparent in the crystallographic structure. The insertion of an α-helical segment into CBR1 in cPLA2 likely confers a greater rigidity to this region. Calcium binding was found to induce a conformational change in CBR1 of PLC-δ1 crystals that moved this loop further apart from CBR3 (42). As we have been unable to grow crystals of the cPLA2 C2 domain in the absence of Ca^{2+}, we cannot estimate the effect of Ca^{2+} on the loop conformation. However, the effect of calcium on structural stabilization of the cPLA2 C2 domain is evident in the calcium-dependent shift of the denaturation temperature from 68 to ≥85 °C.[3] Similar calcium-dependent shifts in denaturation temperature have

[3] S. Fong and M. Bycroft, unpublished data.

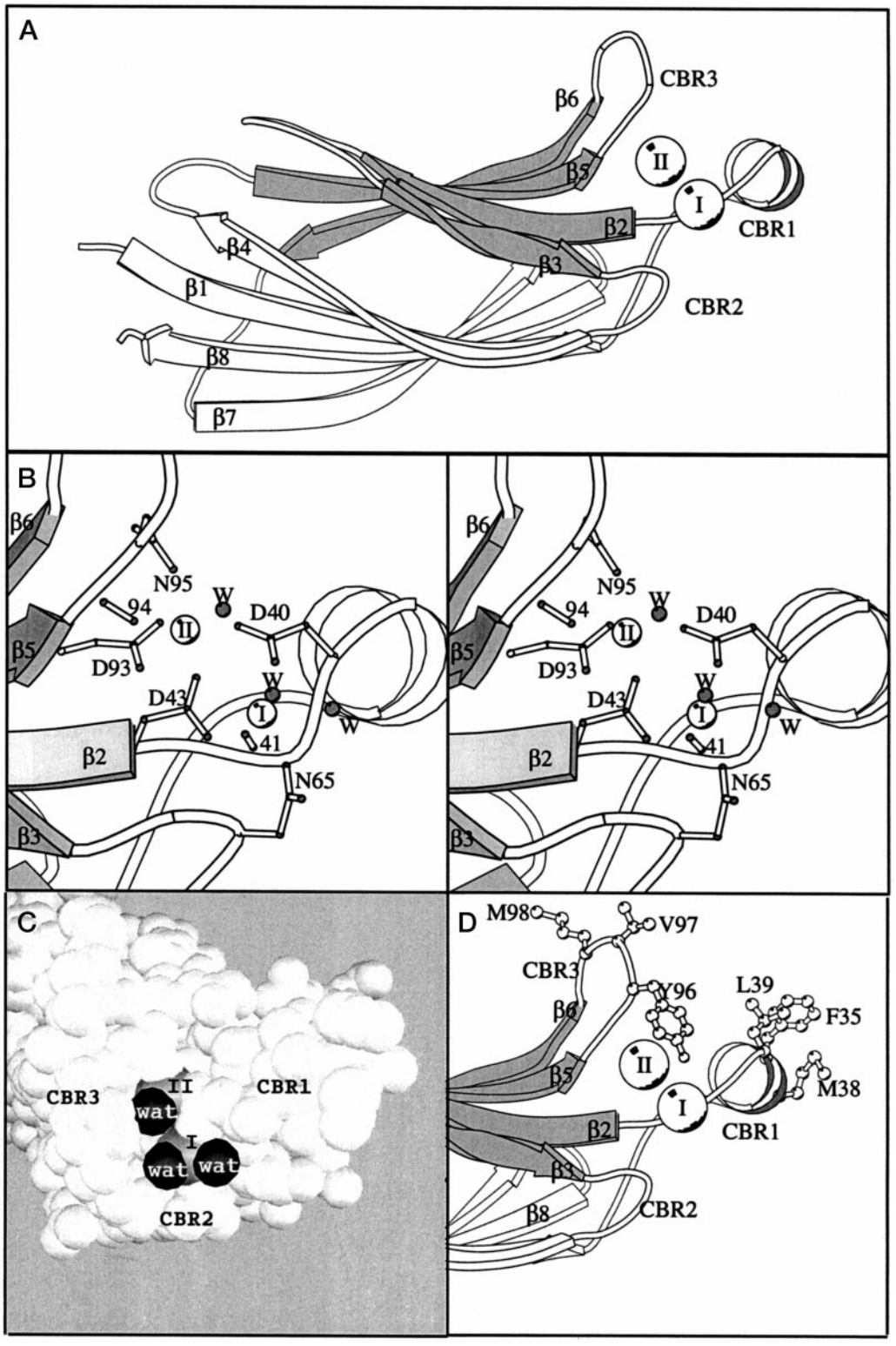

FIG. 1. **A schematic representation of the cPLA$_2$ C2 domain.** *A*, the overall fold of the domain. Sheets I and II of the β-sandwich are colored *gray* and *white*, respectively. The two calcium ions at sites I and II (indicated as *spheres*) are bound between the three loops, CBR1, CBR2, and CBR3. *B*, a stereo view of the CBRs with the calcium ligands illustrated in *ball and stick* representation. The three water molecules (*shaded spheres* labeled *W*) bound to the two calcium ions (*white spheres*) are also illustrated. *C*, the solvent-accessible areas of the calcium ions at sites I and II (*large gray spheres*) are occupied by ordered water molecules (*wat*, *black spheres*). These waters would presumably be displaced if the phosphate moiety of a lipid headgroup interacted directly with the calcium ions. *D*, a view of the CBRs with the hydrophobic residues of CBR1 and CBR3 shown in *ball-and-stick* representation. The figure was made using the programs MOLSCRIPT (71) and GRASP (72).

been observed for the SytI-C2A domain (from 55 to 74 °C) and for PKC-β C2 domain (from 48 to 74 °C) (41).

cPLA2 Has a Preference for Head Groups with Hydrophobic Features—Both CBR1 and CBR3 of cPLA2 have a prominent cluster of hydrophobic residues (Fig. 1*C*, Fig. 4). In CBR1, these hydrophobic residues (Phe-35, Met-38, and Leu-39) are arrayed on the exposed face of the α-helical segment, and in CBR3, the hydrophobic residues (Tyr-96, Val-97, and Met-98) are also

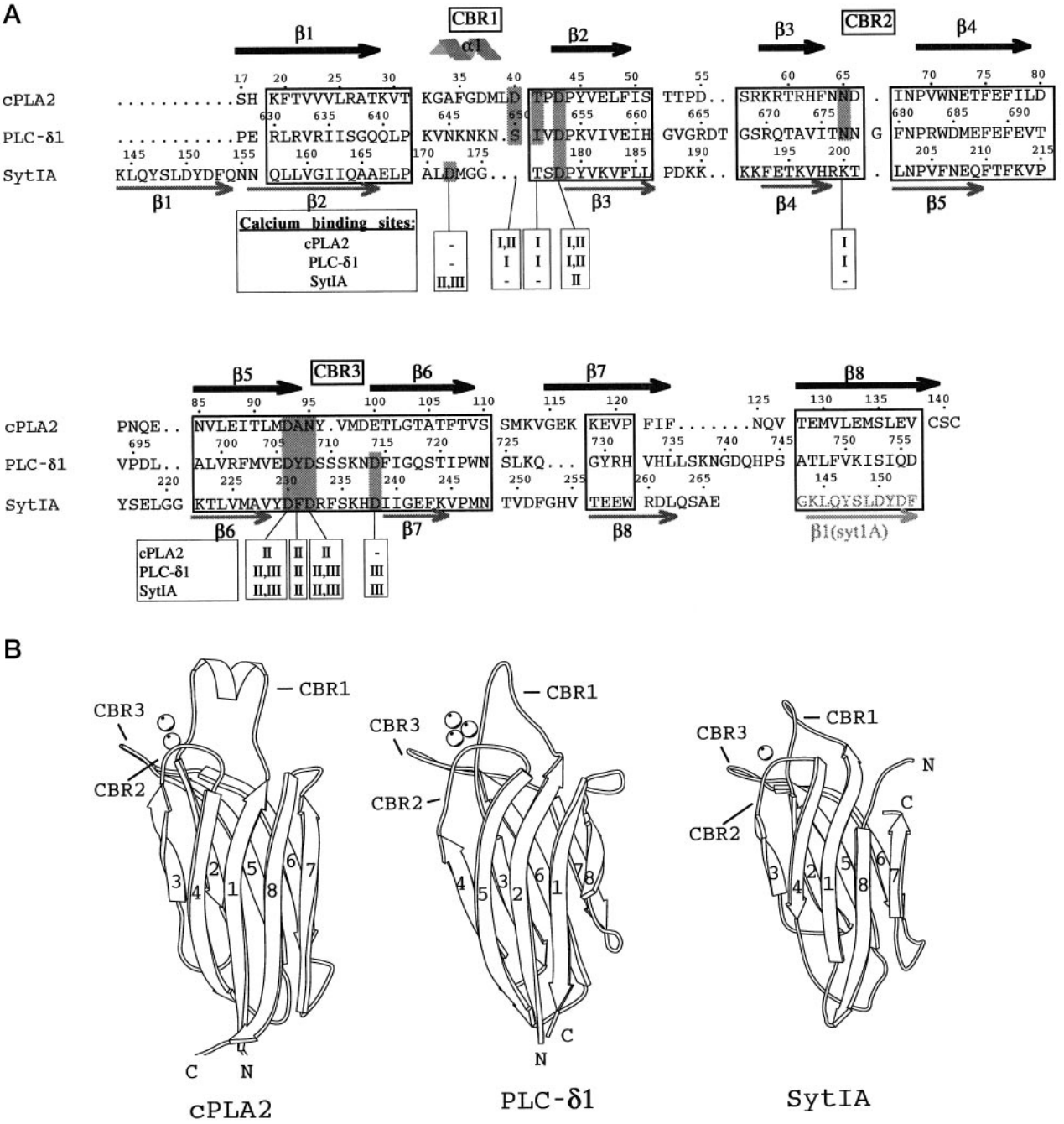

FIG. 2. **A comparison of the three structurally characterized C2 domains.** *A*, a sequence alignment for the C2 domains of cPLA2 (human), PLC-δ1 (rat), and SytI-C2A (rat). The secondary structure elements of $cPLA_2$ are indicated *above* the sequence. Because the topology of SytI-C2A is a circular permutation of cPLA2 and PLC-δ1, the numbering for structurally equivalent strands is different. The *boxed* sequences represent regions that can be structurally superimposed. Residues in *gray-shaded* areas bind calcium or calcium analogues, and the calcium binding sites (I, II, or III) to which the residues contribute are indicated *below* the sequence. *B*, a schematic of the three C2 domain crystal structures with bound metals. One consequence of the differences in topology is that the N and C termini are on opposite ends of the domain.

exposed and include the apex of the loop. The exposed hydrophobic area in these two loops is 780 $Å^2$. This hydrophobic patch may have a significant contribution to the membrane binding of this domain. Indeed, both intact cPLA2 and the cPLA2 C2 domain show calcium-dependent, preferential binding to phospholipids with hydrophobic features of the headgroup such as phosphatidylcholine in preference to phosphatidylserine, phosphatidylinositol (PI) or phosphatidic acid (13, 16, 35). cPLA2 is also known to bind very tightly to lipid vesicles consisting of synthetic phospholipid phosphatidylmethanol, 1,2-dimyristoyl-*sn*-glycero-3-phosphomethanol and 1,2-dioleoyl-*sn*-glycero-3-phosphomethanol (47, 48). Although there are no data on the binding of the isolated cPLA2 C2 domain to these phospholipids, the calcium-dependence of their binding to intact cPLA2 suggests that the site of interaction is in the C2 domain.

High salt concentrations overcome the requirement of cPLA2 for calcium. Activities higher than in the presence of calcium were observed with $(NH_4)_2SO_4$, Na_2SO_4, and NaCl, in proportion to their ability to induce hydrophobic interactions (15, 24, 25). Because the catalytic domain alone cannot hydrolyze liposomal substrates in the presence of high salt, this effect is likely due to C2 domain of cPLA2 (16). This stimulatory effect of high salt concentration on the phospholipid binding is in

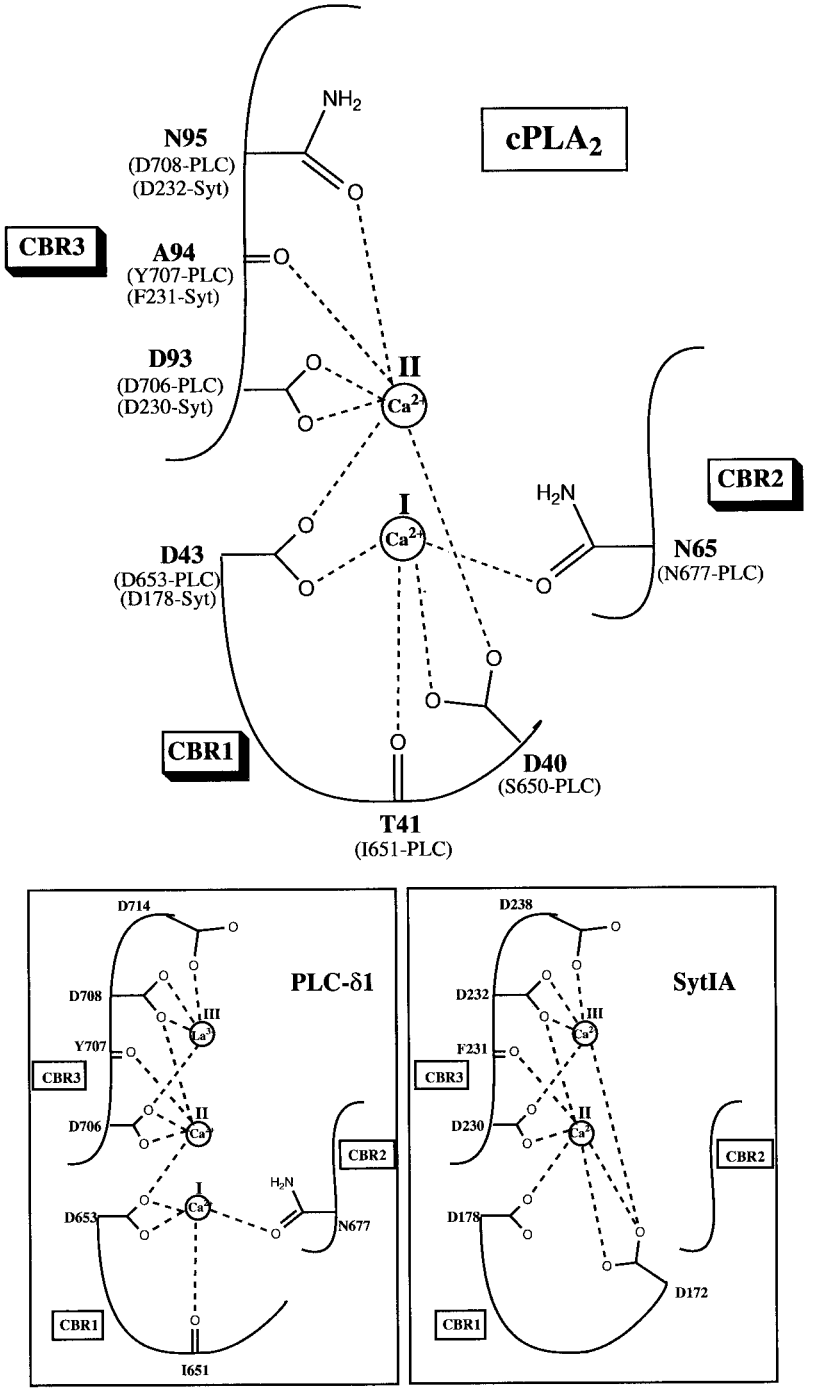

FIG. 3. **A schematic summary of calcium ligation for cPLA$_2$, PLC-δ1, and SytI-C2A domains.** Structural studies of C2 domains suggest three possible calcium binding sites, I, II, and III (38). These diagrams describe the coordination of the calcium and the relationship of binding sites among the three C2 domains.

sharp contrast to the salt effect on the calcium-dependent phosphatidylserine binding of PKC-βII (49). Physiological concentrations of KCl (137 mM) drastically decreased the calcium-dependent, C2 domain-mediated binding of PKC-βII to vesicles, suggesting that electrostatic interactions represent a driving force for this binding (49, 50). Only in the presence of diacylglycerol or phorbol esters, which bind to the C1 domain of PLC-βII and increase membrane affinity 2 or 4 orders of magnitude, respectively, does this enzyme show high affinity, calcium-dependent interaction with phosphatidylserine (51, 52).

A Model for the cPLA2 C2 Domain Interaction with Membranes—The types of residues displayed on the surface of the cPLA2 C2 domain suggest an interaction with membranes such that the hydrophobic CBR3 inserts into the membrane, CBR1 interacts with the hydrophobic portions of the lipid head group (*e.g.* the methylene and methyl groups of a choline moiety), and a patch of basic residues arrayed along strand β3 makes weaker electrostatic interactions with the negatively charged lipid head groups (Fig. 4 and 5). In the presence of bound calcium, the surface of cPLA2 shown in Fig. 4 would become positively charged and would presumably be the surface directed toward the membrane. In PLC-δ1, the analogous surface is exposed in the structure of the intact enzyme, whereas much of the rest of the surface of the domain is involved in interaction with the EF-hand domain and the linker sequence between the catalytic domain and the C2 domain (37, 42, 53, 54).

The insertion of CBR3 into the membrane would probably displace at least two phospholipids (Fig. 5). This could explain a number of observations that phospholipid composition affects calcium-dependent binding of cPLA2 to vesicles. More stable,

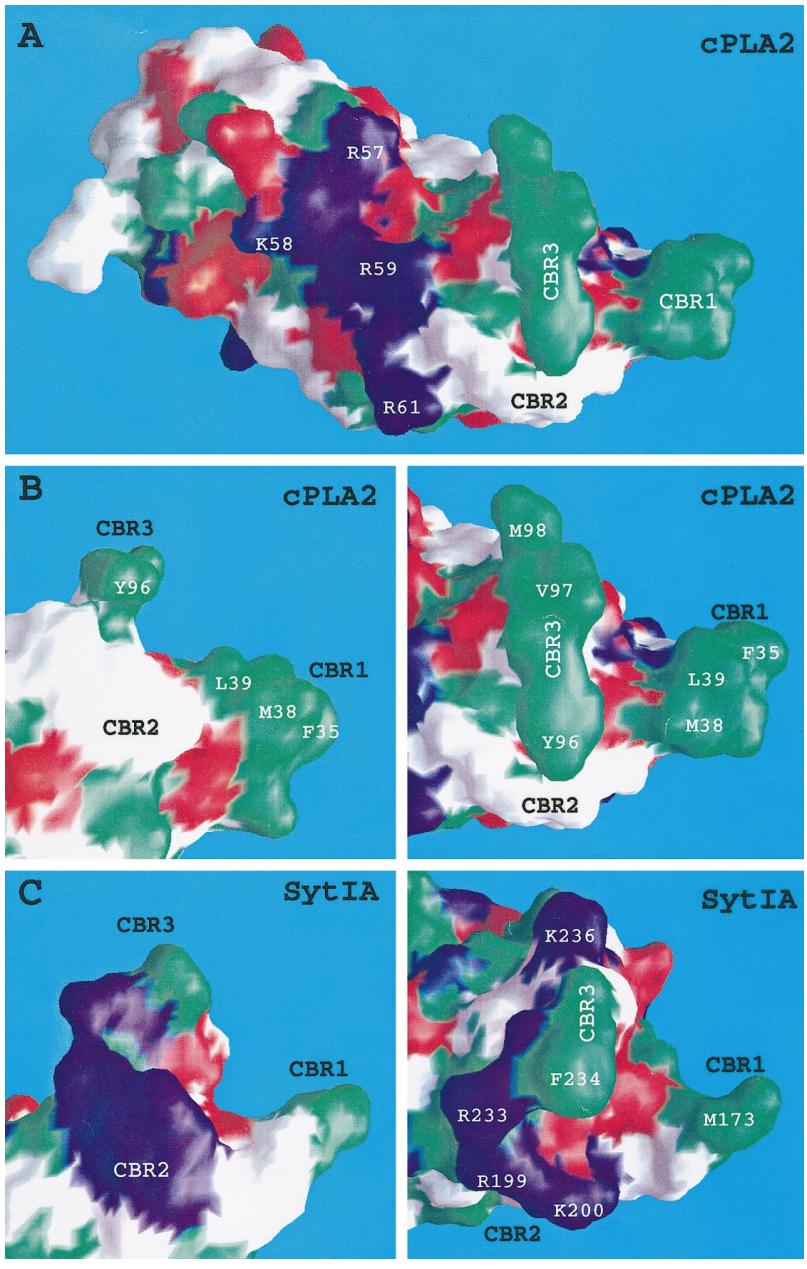

FIG. 4. **A surface representation of cPLA2 C2 domain and a comparison with SytI-C2A.** *A*, the entire domain of cPLA2 oriented to illustrate the strikingly hydrophobic CBRs and a prominent strip of basic residues on strand β3. The residues are colored by type. Basic residues are *blue*, acidic are *red*, and hydrophobic (Ala, Pro, Val, Leu, Ile, Met, Phe, Tyr, and Trp) are colored *green*. *B*, an expanded view of the CBRs in either the same orientation as A (*right*) or rotated 90° around a horizontal axis (*left*). *C*, views of the SytI-C2A domain in orientations equivalent to those shown in *B*. The figures were created with the program GRASP.

calcium-dependent interaction with highly curved sonicated vesicles (phospholipid or membrane) than with natural membranes indicates that head group spacing can have significant effects on the enzyme binding to phospholipids (15). Tight binding of cPLA2 to the vesicles is also enhanced by the presence of free arachidonic acid and lysophosphatidylcholine in the vesicles (55). Diacylglycerol, known to increase the headgroup spacing, promotes activity and vesicle binding of cPLA2 (56), whereas sphingomyelin, which increases packing density in the hydrophobic core and changes the water structure at the interface (57), decreases cPLA2 binding (56). In fact, very similar effects of the packing properties of phospholipids on calcium-dependent binding of the C2 domain from PKC-β has been extensively documented (for the recent reviews, see Refs. 54, 58, and 59), suggesting that in all C2 domains, CBR3 might at least partially penetrate into the membrane. Indeed, structural comparison of cPLA2-C2, PLC-C2, and SytI-C2A domains reveals that the conformation of CBR3 is largely unchanged, despite sequence variation in the loop and different topologies of the domain. Interestingly, the tip of CBR3 in about half of the known C2 domains contains a single hydrophobic residue, whereas the residues surrounding this tip are commonly basic, as seen in the structure of SytI-C2A (Fig. 4, *panel C*) and in sequence alignments for other synaptotagmins, PKC-α,-β,-γ, rasGTPase activating protein, and RSP5. This suggests that a combination of hydrophobic and electrostatic forces may be involved in interactions with phospholipids. The CBR3 loop in cPLA2 is unusually hydrophobic and has no basic residues. A similar character for this loop is also found in unc13(a), phosphatidylserine decarboxylase 2, and PKC-ϵ, -η (for the alignment, see Ref. 35). Furthermore, a hydrophobic nature of CBR1 similar to cPLA2 is also likely to occur in PKC-ϵ and -η, both of which have a long CBR1 with several hydrophobic residues. Using a helical wheel analysis, these residues would cluster on one side of a helix.

The basic residues arrayed along strand β3 of cPLA2 are a common feature of many C2 domains, for example those from conventional PKCs, C2B domain of synaptotagmins and in phosphoinositide 3-kinase (60–62). In these C2 domains, but not in cPLA2, this basic nature of strand β3 continues into CBR2. The importance of basic residues in strand 3 and CBR2 for electrostatic interaction has been documented by mutagen-

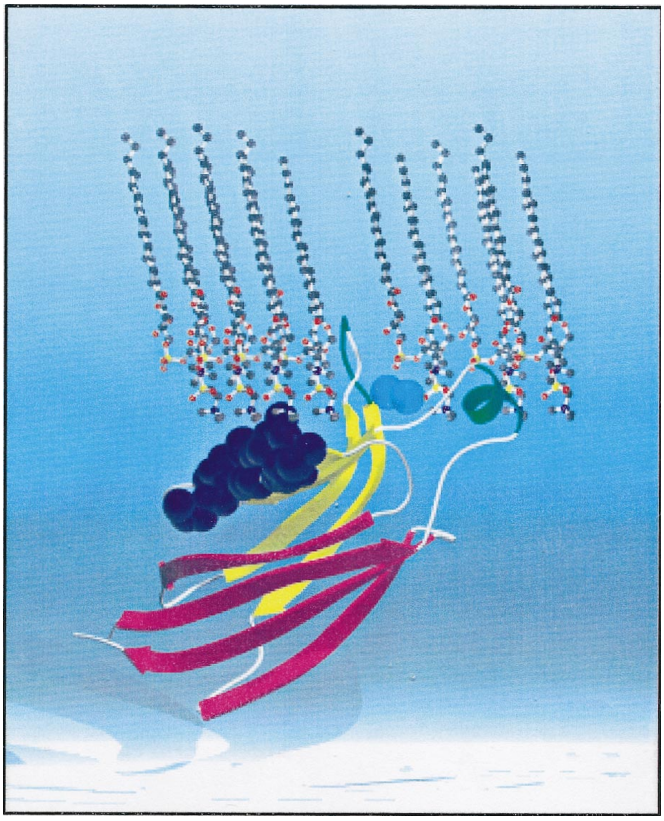

FIG. 5. **A model of the proposed interaction of cPLA2 C2 domain with a phospholipid membrane (rendered with POV-RAY™).** The membrane lipids are taken from a crystal structure of a 1,2-dimyristoyl-*sn*-glycero-3-phosphorylcholine bilayer (73). The domain was approximately oriented so that 1) the hydrophobic tip of CBR3 penetrated into the membrane, displacing 2–3 phospholipids from the membrane, 2) the phosphate group of one phospholipid makes a direct interaction with calcium ions bound in sites I and II, 3) the hydrophobic residues of CBR1 are in the interface region of the membrane and interacting with the methyl groups of the phosphatidylcholine headgroups, and 4) the strip of basic residues along strand β3 shown in the CPK representation (*dark blue spheres*) is near the surface of the membrane layer to facilitate electrostatic interactions with the phospholipid head groups.

esis of these residues in the C2B domain of synaptotagmin IV that completely abolishes inositol 1,3,4,5-tetrakisphosphate binding (61). Opposed to cPLA2 where hydrophobic interactions prevail, C2B domains of synaptotagmins are a prototype for predominantly electrostatic interactions of C2 domains with highly negatively charged phospholipids such as phosphatidylinositol 4,5-bisphosphate and phosphatidylinositol 3,4,5-trisphosphate or their headgroups (61, 63–65).

Hydrophobic-Electrostatic Switch of the cPLA2 C2 Domain—The cPLA2 C2 domain interaction with membranes may be analogous to the hydrophobic-electrostatic switch that modulates reversible membrane binding of several myristoylated proteins such as the myristoylated alanine-rich protein kinase C substrate (MARCKS) or Src (66, 67). In those examples, both the hydrophobic interaction of the myristoyl group with the membrane interior and the electrostatic, surface interaction of a cluster of basic residues with polar head groups of acidic phospholipids are necessary to anchor the proteins to the membrane. In the case of cPLA2, the electrostatic switch is Ca^{2+}, which changes the electrostatic properties of the C2 domain surface, *i.e.* neutralizes a cluster of negative charges in the CBR region and enables membrane binding, whereas in the case of MARCKS peptide, the switch is the phosphorylation of the peptide that introduces negative charges and prevents membrane binding. It is unknown whether calcium directly interacts with the phosphate group of phospholipids or whether it plays only an indirect, electrostatic role by neutralizing the negative charge of the acidic cluster. Our extensive efforts to crystallographically resolve this issue did not succeed. Although we were able to grow the crystals of the C2 domain of cPLA2 in the presence of calcium and a millimolar range of glycerophosphocholine and glycerophosphoserine, there was no structural evidence for binding of these compounds to the C2 domain.

The C2 domain of cPLA2 enables reversible, calcium-regulated binding of the intact enzyme to membranes. The control of this localization provides a powerful regulation of the enzyme activity. Once bound to membranes, cPLA2 could undergo processive catalysis (47, 68), a catalytic mode that has been observed *in vitro* for many enzymes involved in lipid signaling and metabolism in which multiple rounds of hydrolysis occur before the enzyme releases from the interface (69, 70).

Acknowledgments—We thank Zeneca Pharmaceuticals for the clone of intact cPLA2, the staff of beamlines EMBL BW7B, Hamburg and Daresbury synchrotron radiation source stations 7.2 and 9.6, UK, Ed Walker for help in synchrotron data collection, Eric de La Fortelle for advice on SHARP, and Gérard Bricogne for help with BUSTER. We are grateful for the support by the MRC/DTI/ZENECA LINK Program (to R. L. W.). We thank the European Union for the support of synchrotron visits to EMBL Hamburg through the Human Capital and Mobility Programme access to Large Installation Project.

REFERENCES

1. Dennis, E. A. (1994) *J. Biol. Chem.* **269,** 13057–13060
2. Dennis, E. A. (1997) *Trends Biochem. Sci.* **22,** 1–2
3. Murakami, M., Nakatani, Y., Atsumi, G., Inoue, K., and Kudo, I. (1997) *Crit. Rev. Immunol.* **17,** 225–283
4. Sharp, J. D., White, D. L., Chiou, X. G., Goodson, T., Gamboa, G. C., McClure, D., Burgett, S., Hoskins, J., Skatrud, P. L., Kang, L. H., Roberts, E. F., and Kramer, R. M. (1991) *J. Biol. Chem.* **266,** 14850–14853
5. Clark, J. D., Lin, L.-L., Kriz, R. W., Ramesha, C. S., Sultzman, L. A., Lin, A., Y., Milona, N., and Knopf, J. L. (1991) *Cell* **65,** 1043–1051
6. Kramer, R. M. (1994) in *Signal-activated Phospholipases* (Liscovitch, M., ed) R. G. Landes Co.,
7. Kramer, R. M., and Sharp, J. D. (1997) *FEBS Lett.* **210,** 49–53
8. Leslie, C. C. (1997) *J. Biol. Chem.* **272,** 16709–16712
9. Lin, L.-L., Lin, A. Y., and Knopf, J. L. (1992) *Proc. Natl. Acad. Sci. U. S. A.* **89,** 6147–6151
10. Hayakawa, M., Ishida, N., Takeuchi, K., Shibamoto, S., Hori, T., Oku, N., Ito, F., and Tsujimoto, M. (1993) *J. Biol. Chem.* **268,** 11290–11295
11. Gronich, J. H., Bonventre, J. V., and Nemenoff, R. A. (1990) *Biochem. J.* **271,** 37–43
12. Clark, J. D., Milona, N., and Knopf, J. L. (1990) *Proc. Natl. Acad. Sci. U. S. A.* **87,** 7708–7712
13. Wijkander, J., and Sundler, R. (1991) *Eur. J. Biochem.* **202,** 873–880
14. Kramer, R. M., Roberts, E. F., Manetta, J., and Putnam, J. E. (1991) *J. Biol. Chem.* **266,** 5268–5272
15. Wijkander, J., and Sundler, R. (1992) *Biochem. Biophys. Res. Commun.* **184,** 118–124
16. Nalefski, E. A., Sultzman, L. A., Martin, D. M., Kriz, R. W., Towler, P. S., Knopf, J. L., and Clark, J. D. (1994) *J. Biol. Chem.* **269,** 18239–18249
17. Channon, J. Y., and Leslie, C. C. (1990) *J. Biol. Chem.* **265,** 5409–5413
18. Yoshihara, Y., and Watanabe, Y. (1990) *Biochem. Biophys. Res. Commun.* **170,** 484–490
19. Peters-Golden, M., and McNish, R. W. (1993) *Biochem. Biophys. Res. Commun.* **196,** 147–153
20. Glover, S., Bayburt, T., Jonas, M., Chi, E., Leslie, C. C., and Gelb, M. H. (1995) *J. Biol. Chem.* **270,** 15359–15367
21. Schievella, A. R., Regier, M. K., Smith, W. L., and Lin, L.-L. (1995) *J. Biol. Chem.* **270,** 30749–30754
22. Sierra-Honigmann, M. R., Bradley, J. R., and Pober, J. S. (1996) *Lab. Invest.* **74,** 684–695
23. Regier, M. K., DeWitt, D. L., Schindler, M. S., and Smith, W. L. (1993) *Arch. Biochem. Biophys.* **301,** 439–444
24. Zupan, L. A., Kruszka, K. K., and Gross, R. W. (1991) *FEBS Lett.* **284,** 27–30
25. Reynolds, L. J., Hughes, L. L., Louis, A. I., Kramer, R. M., and Dennis, E. A. (1993) *Biochim. Biophys. Acta* **1167,** 272–280
26. Leslie, A. G. W. (1992) *Joint CCP4 and ESF-EACMB Newsletter on Protein Crystallography*, Vol. 26, Daresbury Laboratory, Warrington, United Kingdom
27. Collaborative Computing Project Number 4 (1994) *Acta Crystallogr. Sec. D* **50,** 760–763
28. Sheldrick, G. M. (1990) *Acta Crystallogr. Sec. A* **46,** 467–473
29. de La Fortelle, E., and Bricogne, G. (1997) *Methods Enzymol.* **276,** 472–494
30. Abrahams, J. P., and Leslie, A. G. W. (1996) *Acta Crystallogr. Sec. D* **52,** 30–42
31. Jones, T. A., Zou, J.-Y., Cowan, S. W., and Kjeldgaard, M. (1991) *Acta Crystallogr. Sec. A* **47,** 110–119

32. Murshudov, G. N., Vagin, A. A., and Dodson, E. J. (1997) *Acta Crystallogr. Sect. D* **53,** 240–255
33. Laskowski, R. A., MacArthur, M. W., Moss, D. S., and Thornton, J. M. (1993) *J. Appl. Crystallogr.* **26,** 283–291
34. Read, R. J. (1986) *Acta Crystallogr. Soc. A* **42,** 140–149
35. Nalefski, E. A., and Falke, J. J. (1996) *Protein Sci.* **5,** 2375–2390
36. Sutton, R. B., Davletov, B. A., Berghuis, A. M., Südhof, T. C., and Sprang, S. R. (1995) *Cell* **80,** 929–938
37. Essen, L.-O., Perisic, O., Cheung, R., Katan, M., and Williams, R. L. (1996) *Nature* **380,** 595–602
38. Essen, L.-O., Perisic, O., Lynch, D. E., Katan, M., and Williams, R. L. (1997) *Biochemistry* **36,** 2753–2762
39. Lindqvist, Y., and Schneider, G. (1997) *Curr. Opin. Struct. Biol.* **7,** 422–427
40. Ponting, C. P., and Parker, P. J. (1996) *Protein Sci.* **5,** 162–166
41. Shao, X., Davletov, B. A., Sutton, R. B., Südhof, T. C., and Rizo, J. (1996) *Science* **273,** 248–251
42. Grobler, J. A., Essen, L.-O., Williams, R. L., and Hurley, J. H. (1996) *Nat. Struct. Biol.* **3,** 788–795
43. Davletov, B. A., and Südhof, T. C. (1993) *J. Biol. Chem.* **268,** 26386–26390
44. Kojima, T., Fukuda, M., Aruga, J., and Mikoshiba, K. (1996) *J. Biochem.* (*Tokyo*) **120,** 671–676
45. Fukuda, M., Kojima, T., and Mikoshiba, K. (1996) *J. Biol. Chem.* **271,** 8430–8434
46. Davletov, B. A., and Südhof, T. C. (1994) *J. Biol. Chem.* **269,** 28547–28550
47. Diez, E., Louis-Flamberg, P., Hall, R. H., and Mayer, R. J. (1992) *J. Biol. Chem.* **267,** 18342–18348
48. Bayburt, T., and Gelb, M. H. (1997) *Biochemistry* **36,** 3216–3231
49. Newton, A. C., and Keranen, L. M. (1994) *Biochemistry* **33,** 6651–6658
50. Orr, J. W., and Newton, A. C. (1992) *Biochemistry* **31,** 4667–4673
51. Mosior, M., and Epand, R. M. (1993) *Biochemistry* **32,** 66–77
52. Mosior, M., and Newton, A. C. (1996) *Biochemistry* **35,** 1612–1623
53. Williams, R. L., and Katan, M. (1996) *Structure* (*Lond.*) **4,** 1387–1394
54. Hurley, J. H., and Grobler, J. A. (1997) *Curr. Opin. Struct. Biol.* **7,** 557–565
55. Ghomashchi, F., Schüttel, S., Jain, M. K., and Gelb, M. H. (1992) *Biochemistry* **31,** 3814–3824
56. Leslie, C. C., and Channon, J. Y. (1990) *Biochim. Biophys. Acta* **1045,** 261–270
57. Scarlata, S., Gupta, R., Garcia, P., Keach, H., Shah, S., Kasireddy, C. R., Bittman, R., and Rebecchi, M. J. (1996) *Biochemistry* **35,** 14882–14888
58. Newton, A. C. (1997) *Curr. Opin. Cell Biol.* **9,** 161–167
59. Mosior, M., and Epand, R. M. (1997) *Mol. Memb. Biol.* **14,** 65–70
60. Newton, A. C. (1995) *Curr. Biol.* **5,** 973–976
61. Fukuda, M., Kojima, T., Aruga, J., Niinobe, M., and Mikoshiba, K. (1995) *J. Biol. Chem.* **270,** 26523–26527
62. MacDougall, L. K., Domin, J., and Waterfield, M. D. (1995) *Curr. Biol.* **5,** 1404–1415
63. Fukuda, M., Aruga, J., Niinobe, M., Aimoto, S., and Mikoshiba, K. (1994) *J. Biol. Chem.* **269,** 29206–29211
64. Irvine, R., and Cullen, P. (1996) *Curr. Biol.* **6,** 537–540
65. Schiavo, G., Gu, Q.-M., Prestwich, G. D., Söllner, T. H., and Rothman, J. E. (1996) *Proc. Natl. Acad. Sci. U. S. A.* **93,** 13327–13332
66. McLaughlin, S., and Aderem, A. (1995) *Trends Biochem. Sci.* **20,** 272–276
67. Murray, D., Ben-Tal, N., Honig, B., and McLaughlin, S. (1997) *Structure* (*Lond.*) **15,** 985–989
68. Hanel, A. M., Schüttel, S., and Gelb, M. H. (1993) *Biochemistry* **32,** 5949–5958
69. Carman, G. M., Deems, R. A., and Dennis, E. A. (1995) *J. Biol. Chem.* **270,** 18711–18714
70. Gelb, M. H., Jain, M. K., Hanel, A. M., and Berg, O. G. (1995) *Annu. Rev. Biochem.* **64,** 653–688
71. Kraulis, P. J. (1991) *J. Appl. Crystallogr.* **24,** 946–950
72. Nicholls, A. (1992) *GRASP: Graphical Representation and Analysis of Surface Properties*, Columbia University, New York
73. Pearson, R. H., and Pascher, I. (1979) *Nature* **281,** 499–501